Journal of Materials Chemistry C

PAPER

Cite this: J. Mater. Chem. C, 2014, 2, 9813

Hexacyano octahedral metallic clusters as versatile building blocks in the design of extended polymeric framework and clustomesogens†

Maria Amela-Cortes,[a] Stéphane Cordier,*[a] Nikolay G. Naumov,[b] Cristelle Mériadec,[c] Franck Artzner[c] and Yann Molard*[a]

Received 18th September 2014
Accepted 13th October 2014

DOI: 10.1039/c4tc02098g

www.rsc.org/MaterialsC

Using self-assembling processes to generate hybrid organic inorganic materials allows the control of their structuration at the nanometric scale. We describe in this work the synthesis, liquid crystal and photophysical properties of $[M_6Q^i{}_8(CN)^a{}_6]^{n-}$ (M = Mo, Re; Q^i = Br, Se; n = 2, 3 or 4) cluster anionic units containing clustomesogens. A new and efficient synthetic route was developed to synthesize the $[Mo_6Br^i{}_8(CN)^a{}_6]^{2-}$ building block that is stable in water solution and that could be crystallized as the porous [*trans*-$Cd(H_2O)_2$][$Mo_6Br^i{}_8(CN)^a{}_6$]. Hybrids were obtained by a metathesis reaction with a specifically designed organic cation. Their self-assembling abilities can be tailored by playing with the charge of the inorganic building blocks going from a nematogenic behaviour, which is particularly rare for ionic mesomorphic material, to the formation of layered structures. The intrinsic properties (luminescence or magnetism) of transition metal clusters are well retained in the hybrid matrices. The nanostructuration of the material influences its ability to emit light despite the isotropy of the emissive nanocluster. Finally, we demonstrate that the magnetic $[Re_6Se_8CN_6]^{3-}$ can be reduced into the luminescent $[Re_6Se_8CN_6]^{4-}$ upon heating at 150 °C. These hybrid materials show promising prospects in the field of luminescent material.

1. Introduction

Hybrid materials in which organic and inorganic components are intimately mixed constitute an important class of materials in a stage of rapid development. Their physical and chemical properties cannot be described as the sum of each component's individual properties as synergistic effects may occur and contribute to create new behaviours or enhanced properties. Therefore, the field of hybrid materials has become an intense field of investigations mixing chemistry and physics and gives rise to many materials with applications in optics, microelectronics, batteries, biology, photovoltaics, medicine, *etc*.[1] A major challenge in this field, beside the fact that organic and inorganic components should not segregate within the material, is to control the hybrid architecture at the molecular level. Several strategies now enable the assembling of structurally well-defined nanocomponents into hierarchically organized hybrid architectures. Among them, self-assembling seems the most promising way to control the material structuration as it uses a bottom up approach. In that way, liquid crystal (LC) nanoscience, is an emerging field in the world of hybrid materials, which main goal is to control the self-assembling ability of some hybrid systems to tailor the molecular arrangement at the molecular scale.[2] Using such strategy allows taking advantage of the "self-healing" ability of LC materials suppressing nearly all structural defects that can exist in the material at the macroscopic scale. In such systems, the self-assembling abilities are predominantly governed by the organic components while the inorganic components add one or more functionalities to the final material. $A_n[M_6Q^i{}_8X^a{}_6]$ (A = alkali; M = Mo, Re, W; Q = chalcogen/halogen, X = halogen) octahedral transition metal cluster compounds,[3] obtained *via* high temperature synthesis, are an attractive class of nanosized building block precursors to develop such types of hybrid material.[4] $[M_6Q^i{}_8X^a{}_6]^{n-}$ (n = 2, 3 or 4) units are characterized by a rigid $(M_6Q^i{}_8)^{m+}$ cluster core (m = 4, 5 or 6) with interesting structural, electronic and photochemical properties related to the number of metallic electrons available for metal–metal bonds (VEC).[5,6] Among these properties we can cite phosphorescence in the red-NIR with lifetimes in the range of several tenths of microseconds, high

[a]Université de Rennes 1, ENSC Rennes – CNRS UMR 6226, Institut des Sciences Chimiques de Rennes, Campus de Beaulieu, CS 74205, 35042 Rennes Cedex, France. E-mail: yann.molard@univ-rennes1.fr; stephane.cordier@univ-rennes1.fr

[b]Nikolaev Institute of Inorganic Chemistry, Siberian Branch of the Russian Academy of Sciences, 3 Acad. Lavrentiev pr., 630090 Novosibirsk, Russia

[c]Université de Rennes 1, Institut de Physique de Rennes, UR1-CNRS UMR 6251, Campus de Beaulieu, CS 74205, 35042 Rennes Cedex, France

† Electronic supplementary information (ESI) available: Additional presentation of structural data of $Cd(H_2O)_2[Mo_6Br^i{}_8(CN)^a{}_6]$, UV-vis spectra of **2**, **3** and **4**, EPR spectrum of **3**, temperature dependent small angle diffractograms and DSC thermograms, temperature variable luminescence spectra of $KCs_3Re_6Se_8(CN)_6$. See DOI: 10.1039/c4tc02098g

quantum yields, large Stokes-shifts, reversible one-electron oxidation or electroluminescence.[5–7] Within the solid, the charge balance of discrete $[M_6Q^i{}_8X^a{}_6]^{n-}$ units is generally assumed by alkali or divalent cations. However, the ceramic-like behaviour (brittle and low plasticity) in the solid state of such inorganic phosphor strongly limits their potential use in the design of functional devices, commanding new strategies of integration to be explored.

$A_n[M_6Q^i{}_8X^a{}_6]$ inorganic salts (A = alkali or divalent cation)[8,9] become fairly soluble in organic media after a cationic metathesis reaction which consists of replacing the inorganic counter cations by organic ones.[9,10] This solubilisation allows their direct integration in functional nanomaterials and surfaces[11] or their modification with organic moieties giving hybrid building blocks where organic ligands are orthogonally arranged around the cluster core.[9,12,13] Moreover, these nanometer sized inorganic units seems to focus the interest of scientists with different backgrounds. For instance, R. Ramirez-Tagle *et al.* recently showed that tumoral cells were more sensitive to Re_6 clusters-induced cell death than healthy cells and therefore that they could be useful for cancer diagnostics, localization of tumors, and may enable the observation through fluorescence of tumor regression during treatment.[14] $[Mo_6Br_{14}]^{2-}$ clusters which have higher quantum yield of phosphorescence than their Re cluster equivalent have been incorporated in polymers to give easily processable deep red emitters that can sensitize the infrared emission of Er^{3+}.[15] Alone or combined to graphene oxide and gold nanoparticles, $[Mo_6Br_8(N_3)_6]^{2-}$ cluster shows excellent photocatalytic performances for the degradation of rhodamine B under visible light irradiation whereas $[Mo_6Br^i{}_8Br^a{}_6]^{2-}$ exhibits interesting potential for the sun light photo-reduction of CO_2.[16] The massive Stokes-shift of $Cs_2Mo_6Cl_{14}$ clusters allows the design of transparent solar cell concentrators with high quantum efficiency as depicted by Zhao *et al.*[17] Depending on the nature of the constituting metal atoms, inner (Q^i) and apical (X^a) ligands, the cluster charge and the value of the oxidation potential can be adjusted at will. For instance, Re_6 based clusters of formula $[Re_6Se_8CN_6]^{n-}$ (n = 3 and 4) show a low oxidation potential and can be reversibly switched from an orange coloured form (n = 4, VEC = 24) with red-NIR luminescence properties to a stable and magnetic green coloured species (n = 3, VEC = 23).[18] Such modification can be easily implemented by both chemical and electrochemical oxidation, that can be useful for colour, luminescence and magnetic switching. In order to incorporate transition metal clusters in liquid crystal matrices, we previously described two strategies: the covalent approach that consists in grafting mesogenic groups onto the apical position of clusters and the ionic self-assembling approach (ISA)[19] in which the cluster inorganic counter cations are replaced by promesogenic organic ones.[20–22] In this last case, chemically inert hexacyano cluster building blocks were used to avoid the formation of by-products during cationic exchanges thanks to the strong covalent Re–CN bonds. Thus, we showed that by combining a dialkyldimethylammonium cation containing two cyanobiphenyl (CB) terminated decyloxy chains with an anionic $[Re_6Se_8(CN)_6]^{3-}$ cluster, a thermotropic lamellar smectic A liquid crystal phase was observed. The combination of the same cation with $[Re_6Se_8(CN)_6]^{4-}$ did not allow the formation of a well-defined thermotropic LC phase but both compounds ($\mathbf{3}^-$ and $\mathbf{4}^-$) showed lyotropic behaviour. Motivated by these results we were interested in tuning the liquid crystal behaviour of our hybrid materials by modifying the volumic ratio between the organic and inorganic parts of the hybrid. To do so, we designed a new promesogenic cation (Kat^+, compound **1**) bearing three alkoxy chains terminated by CB units allowing us to increase the maximal mesogenic density around Re_6 clusters from 8 CB to 12 CB as compared to our previous results. To reduce the mesogenic density around the cluster, keeping constant the nature of the organic cation and the volume of the inorganic cluster anion, we developed a straightforward method to synthesize a water soluble inorganic precursor containing doubly charged $[M_6L_8(CN)_6]^{2-}$ cluster building block, namely $K_2[Mo_6Br_8(CN)_6]$. Structural data on this building block were obtained after crystallization with Cd^{2+} to form [*trans*-$Cd(H_2O)_2$] $[Mo_6Br^i{}_8(CN)^a{}_6]$ inorganic compound whose structure is strongly related to that of Cs_2[*trans*-$Cd(H_2O)_2$][$Re_6S^i{}_8(CN)^a{}_6$].[23] Using $[Mo_6Br_8(CN)_6]^{2-}$, $[Re_6Se_8(CN)_6]^{3-}$, and $[Re_6Se_8(CN)_6]^{4-}$, we tailored the mesogenic density around the octahedral cluster building blocks from 6 to 12 CB units and thus the molecular volumic organic/inorganic ratio. Along with the synthesis and full characterizations of $[Mo_6Br_8(CN)_6]^{2-}$ building block, we present in this work a new series of clustomesogens with self-assembling abilities that are controlled by the charge of the inorganic entities they contained. We show how LC properties can be tuned by playing with the mesogenic density around an octahedral metallic cluster, and in particular, we describe the first nematic hybrid compound obtained *via* ISA strategy and bearing CB units. Optical studies are reported and highlight the influence of the nanostructuration on the luminescence behaviour of these hybrid materials.

2. Experimental

2.1. Experimental techniques

NMR spectra were recorded on a Bruker Avance 400P. All signals were referenced to the methyl signals of TMS at $\delta = 0$ ppm. UV-vis absorption measurements were performed on a Varian Cary 5000 UV-vis-NIR spectrophotometer. Luminescence spectra were recorded either on a Fluorolog-3™ fluorescence spectrometer (FL3-22, Horiba Jobin Yvon) or with an ocean optic QE6500 photodetector mounted on the polarized optical microscope described below. Elemental Analyses were performed in the CRMPO with a Microanalyser Flash EA1112 CHNS/O Thermo Electron. Energy dispersive spectroscopy (EDS) was performed on a JEOL 6400 scanning electron microscope equipped with a XEDS Oxford field spectrometer. Polarized optical Microscopy and temperature dependent luminescence measurements were realized with a Nikon 80i polarized microscope equipped with a Linkam LTS420 hot stage, a Nikon Intensilight irradiation source, a Nikon DS-FI2 digital camera and an ocean optics QE6500 photodetector connected by optical fibre. Two optical filters were used to select

the excitation wavelength: either with a bandwidth: 330–380 nm or with a bandwidth 380–420 nm. DSC measurements were realized at 10 K min^{-1}, unless otherwise stated, with a DSC 200 F3 Maia NETSCH apparatus. X-ray data collection for the structural resolution of [*trans*-$Cd(H_2O)_2$][$Mo_6Br^i{}_8(CN)^a{}_6$] was performed with an APEXII, Bruker-AXS diffractometer using Mo-K_α radiation ($\lambda = 0.71073$ Å). Small Angle X-ray spectra for the characterization of clustomesogens are given as the scattering intensity *versus* the wavevector transfer $q = 4\pi \sin\theta/\lambda$ ($Å^{-1}$). X-ray scattering experiments were performed using an FR591 Bruker AXS rotating anode X-ray generator operated at 50 kV and 50 mA with monochromatic Cu K_α radiation ($\lambda = 1.541$ Å) and point collimation. X-ray patterns were collected with a Mar345 Image-Plate detector (Marresearch, Norderstedt, Germany). The monochromatic Cu K_α radiation ($\lambda = 1.541$ Å) was directed with a 350 μm × 350 μm focal spot at 320 mm by a double reflection on an elliptic cross multilayer Montel mirror (Incoatec, Geesthacht, Germany). The beam was defined under vacuum by four motorized carbon–tungsten slits (JJ-Xray, Roskilde, Denmark) positioned in front of the mirror (500 μm × 500 μm). Four additional guard slits (600 μm × 600 μm) were placed at the focal point with a 220 mm slit separation distance. The flux after the output mica windows was 3×10^8 photons per s. A 2 mm diameter square lead beam stop was placed under a vacuum at 270 mm; afterward, the sample and the detector were positioned at 420 mm. The X-ray patterns were therefore recorded for a range of reciprocal spacing $q = 4\pi \sin\theta/\lambda$ from 0.03 to 1.56 $Å^{-1}$, where θ is the diffraction angle. The repetition distances $d = 2\pi/q$ should be between 200 and 4.0 Å. The samples were placed into 1.5 mm glass capillaries (Glass W. Müller, Germany) and introduced into a homemade capillary holder, which can maintain up to 20 capillaries at a controlled temperature. We used the programs Fit 2D and IgorPro to treat the data.[24]

2.2. Crystallographic analyses

Further details on the crystal-structure investigations may be obtained from the Fachinformationzentrum Karlsruhe, D-76344 Eggenstein-Leopoldshafen, Germany, on quoting the depository number CSD-427637 (http://www.fiz-karlsruhe.de/). Formula: $C_6Br_8CdH_4Mo_6N_6O_2$, sample size = 0.05 × 0.08 × 0.120 mm^3, $\lambda = 0.71069$ Å (Mo K_α), Bruker AXS APEX-II diffractometer, $T = 293(2)$, orthorhombic system, space group *I mcm* (N° 74), $M_r = 1519.47$ g mol^{-1}, $\rho_{calc} = 3.500$ g cm^3, $a = 10.6047(3)$ Å, $b = 13.7982(5)$ Å, $c = 19.7050(7)$ Å, $V = 2883.3$ $Å^3$ ($c/a = 1.858$), $Z = 4$, SORTAV absorption correction, SHELXL-2014, 2266 independent reflections, 81 parameters, (Sheldrick, 2014), $R_1 = 3.44[I > 2\sigma(I)]$, $wR_2 = 7.91$, GooF = 1.088, largest difference peak and hole +1.96 and −1.76 e $Å^{-3}$. Important interatomic distances (Å). Opposite N1–N1: 10.4294(3) and N2–N2: 10.4665(2); Mo1–Mo2: 2.6409(5); Mo1–Mo2: 2.6410(5) 2.6429; Mo2–Mo2: 2.6406(7); Mo2–Mo2: 2.6439(7); average Mo–Mo: 2.6420; NC: 1.116; Mo–C: 2.221–2.232(6); CN: 1.116(8)–1.150(6); MoBri: 2.5929(5)–2.5929–2.6027(5); Cd–N2: 2.289(5); Cd–O: 2.405(2)–2.423(9); O1–N1: 2.738 (9); O2–Br3 3.663(8) (×2); O2–Br3: 3.661(2) (×2); N1–Br1: 3.381 (×2), C1–Br1: 3.475 (×2).

2.3. Synthesis

$MoBr_2$, $KCs_3[Re_6Se_8(CN)_6]$ and the chain 4′-cyano-4(ω-bromodecyloxy)biphenyl was prepared according to a described procedure.[22,25] Starting materials were purchased from Acros Organics, Alfa-Aesar or Aldrich, and used without further purification unless otherwise stated.

$K_2[Mo_6Br^i{}_8(CN)^a{}_6]$. 300 mg of KCN were dissolved in 10 ml of methanol in a Schlenk tube. Then, 1 g of $MoBr_2$ prepared *via* gas solid reaction were added to the mixture and stirred 24 h under reflux. The resulting brown solution was filtered and methanol was evaporated almost to dryness. Then dichloromethane was added to separate the excess of KCN and KBr. The solution was separated by decantation and evaporation. Just before dryness, 0.5 ml of methanol was used to dissolve the compounds and dichloromethane was added to remove the remaining KCN and KBr by precipitation. This operation was repeated 3 times and single crystals suitable for structural analysis by X-ray diffraction were obtained as follow: 50 mg (3.45×10^{-5} mol) of $K_2[Mo_6Br^i{}_8(CN)^a{}_6]$-10MeOH were dissolved in 1.5 ml of methanol and layered on 1.5 ml water solution containing 1.5 equivalent of cations. Suitable single crystals were of $Cd(H_2O)_2[Mo_6Br^i{}_8(CN)^a{}_6]$ for X-ray diffraction were after two weeks of slow diffusion.

ω-[4-(4′-Cyanobiphenylyl)oxy]decyl]methylammonium bromide (Kat–Br) (1). To a solution of 4′-cyano-4(ω-bromodecyloxy)biphenyl (447 mg, 1.08 mmol) in 3 mL of ethanol was added anhydrous K_2CO_3 (373 mg, 2.7 mmol) and a 2.0 M solution of methylamine in THF (11.4 mg, 0.36 mmol). The mixture was heated in a close reaction vessel for 24 h at 95 °C. The reaction was then cooled to room temperature and the solvent evaporated under vacuum. Dichloromethane was added and the solution filtered off. The dichloromethane was evaporated under vacuum and the product purified by silica gel chromatography (DCM : MeOH from 1 : 0 to 96 : 4). ^{1}H-NMR (300 MHz, $CDCl_3$): 1.34–1.39 (36H, m), 1.71–1.83 (12H, m), 3.34 (3H, s), 3.44 (6H, m), 4.00 (6H, t, $J = 6.6$ Hz), 6.99 ($6H_{Ar}$, d, $J = 8.7$ Hz), 7.53 ($6H_{Ar}$, d, $J = 8.7$ Hz), 7.66 ($12H_{Ar}$, q, $J = 8.4$ Hz). ^{13}C-NMR (100 MHz, $CDCl_3$): 22.5–29.3 (–CH_2–), 48.9 (–N–CH_3), 61.6 (N–CH_2), 68.1 (O–CH_2), 109.9 (C^{Ar}–CN), 1115.0 (C^{Ar}) 119.1 (CN), 127.0 (C^{Ar}), 128.3 (C^{Ar}), 131.2 (C^{Ar}), 132.5 (C^{Ar}), 145.2 (C^{Ar}), 159.8 (C^{Ar}–O). Mass-spectrometry: ESI: $[C_{70}H_{87}N_4O_3]^+$: 1031.67. CHN: found: C, 73.29; H, 7.80; N, 4.76% $C_{70}H_{87}N_4O_3$ Br·$2H_2O$ requires C, 73.21; H, 7.99; N, 4.88.

$Kat_2[Mo_6Br_8(CN)_6]$ (2). To a methanol solution of $K_2Mo_6Br_8(CN)_6$ (0.097 g, 0.067 mmol) was added a solution of the ammonium salt in hot ethanol (0.150 g, 0.135 mmol). The reaction was heated for one hour at reflux to assure complete precipitation of the compound. The product was purified by washing three times in hot water and three times in hot ethanol and further dried under vacuum. ^{1}H-NMR (300 MHz, $CDCl_3$): 1.34–1.39 (72H, m), 1.71–1.83 (24H, m), 3.21 (6H, s), 3.36 (12H, m), 4.00 (12H, t, $J = 6.6$ Hz), 6.99 ($12H_{Ar}$, d, $J = 8.7$ Hz), 7.53 ($12H_{Ar}$, d, $J = 8.7$ Hz), 7.66 ($12H_{Ar}$, q, $J = 8.4$ Hz). ^{13}C-NMR (100 MHz, $CDCl_3$): 22.5–29.4 (–CH_2–), 49.0 (N–CH_3), 62.0 (N–CH_2), 68.1 (O–CH_2), 109.9 (C^{Ar}–CN), 115.3 (C^{Ar}), 119.1 (CN), 127.0 (C^{Ar}), 128.3 (C^{Ar}), 131.2 (C^{Ar}), 132.5 (C^{Ar}), 145.2 (C^{Ar}),

159.8 (C^{Ar}–O). CHN: found: C, 49.86; H, 5.10; N, 4.95% $Mo_6Br_8C_{146}H_{174}N_{14}O_6$, $5H_2O$ requires C, 49.73; H, 5.26; N, 5.56. EDAX: no K; Mo: 48.55; Br: 48.56.

$Kat_3[Re_6Se_8(CN)_6]$ (3). To an orange water solution of $KCs_3[Re_6Se_8(CN)_6]$ (0.094 g, 0.04 mmol) was added two drops of liquid bromine. The solution was stirred for 10 min at 25 °C. A solution of the ammonium salt in hot ethanol (0.150 g, 0.135 mmol) was then added and the solution stirred at reflux for 1 hour. After that dichloromethane was added and the organic layer was collected, dried over $MgSO_4$, and the solvent evaporated. The product was purified by successive precipitations in hot ethanol. ^{1}H-NMR (400 MHz, $CDCl_3$): 1.34–1.39 (108H, m), 1.71–1.83 (36H, m), 3.27 (27H, m), 4.00 (18H, t, $J = 6.6$ Hz), 6.99 ($18H_{Ar}$, d, $J = 8.7$ Hz), 7.53 ($18H_{Ar}$, d, $J = 8.7$ Hz), 7.66 ($36H_{Ar}$, q, $J = 8.4$ Hz). ^{13}C-NMR (100 MHz, $CDCl_3$): 22.2–28.6 (–CH_2–), 63.0 (N–CH_2), 67.4 (O–CH_2), 108.9 (C^{Ar}–CN), 1114.2 (C^{Ar}) 118.1 (CN), 126.0 (C^{Ar}), 127.3 (C^{Ar}), 130.2 (C^{Ar}), 131.6 (C^{Ar}), 144.2 (C^{Ar}), 158.8 (C^{Ar}–O). CHN: found: C, 51.84; H, 5.38; N, 4.88% $Re_6Se_8C_{216}H_{261}N_{18}O_9$ requires C, 51.75; H, 5.45; N, 5.03). EDAX: no K, no Cs, no Br; Re: 52.28; Se: 46.35.

$Kat_4[Re_6Se_8(CN)_6]$ (4). A solution of the ammonium salt (0.150 g, 0.135 mmol) in hot ethanol was added to an orange solution of $KCs_3[Re_6Se_8(CN)_6]$ (0.08 g, 0.033 mmol) in hot water. The product precipitated and the mixture was heated for one hour. The orange precipitate was washed three times with water and three times with hot ethanol and dried under vacuum. ^{1}H-NMR (400 MHz, $CDCl_3$): 1.34–1.39 (144H, m), 1.71–1.83 (48H, m), 3.18 (24H, m), 3.20 (12H, s), 4.00 (24H, t, $J = 6.6$ Hz), 6.99 ($24H_{Ar}$, d, $J = 8.7$ Hz), 7.53 ($24H_{Ar}$, d, $J = 8.7$ Hz), 7.66 ($48H_{Ar}$, q, $J = 8.4$ Hz). ^{13}C-NMR (100 MHz, $CDCl_3$): 22.2–28.6 (–CH_2–), 63.0 (N–CH_2), 67.4 (O–CH_2), 108.9 (C^{Ar}–CN), 1114.2 (C^{Ar}), 118.1 (CN), 126.0 (C^{Ar}), 127.3 (C^{Ar}), 130.2 (C^{Ar}), 131.6 (C^{Ar}), 144.2 (C^{Ar}), 158.8 (C^{Ar}–O). CHN: found: C, 56.92; H, 5.79; N, 4.74% $Re_6Se_8C_{286}H_{348}N_{22}O_{12}$ requires C, 56.92; H, 5.81; N, 5.11. EDAX: no bromine, cesium or potassium; Re: 51.54; Se: 51.54.

3. Results and discussion

3.1. Synthesis and characterizations of octahedral $[M_6L^i_8(CN)^a_6]^{n-}$ cluster building blocks precursors

As stressed above, among all $[M_6Q^i_6X^a_6]^{n-}$ building blocks, hexacyano $[M_6L^i_6(CN)^a_6]^{n-}$ clusters were chosen because of the strong covalent M–CN bonds that afford a chemically inert behaviour. Indeed, it was shown previously that Re_6 metallic clusters bearing halogen atoms or hydroxy groups in apical positions can easily react with solvent molecules or be protonated in water, which for this study would lead to non-defined charged inorganic moieties.[12,26] On the other hand, except $[Mo_6Br^i(N_3)]^{2-}$ cluster units, $[Mo_6Br^iX^a_6]^{2-}$ are known to rapidly form in water insoluble hydroxo complexes. Three different clusters namely $[Mo_6Br_8(CN)_6]^{2-}$, $[Re_6Se_8(CN)_6]^{3-}$, and $[Re_6Se_8(CN)_6]^{4-}$, differing in the charge were used for this study. It is worth noting that if the chemistry of face-capped $[Re_6Q^i_8(CN)^a_6]^{4-}$ rhenium cyanide (Q = S, Se and Te) and that of edge-bridged $[Nb_6Q^i_{12}(CN)^a_6]^{n-}$ (Q = Cl or Cl and O) are rather well developed, almost nothing is known about $[Mo_6Q^i_8(CN)^a_6]^{4-}$ (Q = Br, Br/S or Br/Se) cluster units. For the present work, it was mandatory to investigate a new and straightforward method to obtain $[Mo_6Br^i_8(CN)^a_6]^{2-}$ cluster associated with alkali earth counter cations. Indeed, the preparation of clustomesogens by the ionic approach needs this type of precursor as hybrids are obtained by a metathesis reaction between the alkali cluster salt and a functional organic salt. The preparation of $[Mo_6Br^i_8(CN)^a_6]^{2-}$ units was first reported by Preetz using a multistep procedure starting from $(n\text{-}Bu_4N)_2[Mo_6Br^i_8Br^a_6]$.[27] The reported yield was 30% and no crystal data were reported for this salt. A similar method was used by the same authors to prepare single crystals of $(Ph_4P)_2[Mo_6Br^i_8(CN)^a_6]\text{-}4H_2O$ (Ph_4P = tetraphenylphosphonium) suitable for X-ray diffraction investigation. The reaction was performed in DMF and the reported yield was roughly 60%. As a more efficient route was necessary to prepare a water soluble $[Mo_6Br^i_8(CN)^a_6]^{2-}$ precursor, we implemented a similar method than those reported for the synthesis of $[Nb_6Cl^i_{12}(CN)^a_6]^{4-}$, $[Nb_6Cl^i_9O^i_3(CN)^a_6]^{5-}$ and $[Mo_6Br^i_6Q^i_2(CN)^a_6]^{4-}$ units.[28] It was obtained by interaction of $MoBr_2$ solid state inorganic cluster precursors with a KCN solution (see Experimental section). Although $K_2[Mo_6Br^i_8(CN)^a_6]$ is highly soluble and stable in water and methanol, our numerous attempts to obtain single crystals suitable for X-ray diffraction measurements remained unsuccessful. Therefore, we tried another strategy by crystallizing $[Mo_6Br^i_8(CN)^a_6]^{2-}$ with divalent elements such as Pb^{2+}, Cd^{2+} and Mn^{2+}. Single crystals were then obtained by slow diffusion of an aqueous solution containing the divalent ions onto a methanolic solution of $K_2[Mo_6Br^i_8(CN)^a_6]$. By this technique, only single crystals of $Cd(H_2O)_2[Mo_6Br^i_8(CN)^a_6]$ were found to be suitable for X-ray diffraction. Other divalent elements yielded too small single crystals or yellow precipitates.

3.2. Structural description of $Cd(H_2O)_2[Mo_6Br^i_8(CN)^a_6]$

It is the first time that the stability of $[Mo_6Br^i_8(CN)^a_6]^{2-}$ in aqueous solution is reported. This is an important finding because it opens a new field of research in cluster chemistry, for instance to build extended polymeric frameworks with controlled dimensionality as already developed with rhenium and niobium. The added value of $[Mo_6Br^i_8(CN)^a_6]^{2-}$ cluster units compared to $[Re_6Q^i_8(CN)^a_6]^{4-}$ rhenium and $[Nb_6Cl^i_{12}(CN)^a_6]^{4-}$ niobium cyanides[29] is that it should be possible to obtain neutral porous tridimensional frameworks by complexation of this building block with divalent elements. The complexation reaction of $[Mo_6Br^i_8(CN)^a_6]^{2-}$ unit with divalent element should lead to the formation of three dimensional frameworks with structures strongly related to that of Prussian Blue family as for instance ferri–ferricyanide, $Fe[Fe(CN)_6]\text{-}xH_2O$ or ferro–ferricyanide $Fe_4[Fe(CN)_6]_3$ and many other derivatives.[30] This hypothesis is supported by the fact that such Prussian blue derivatives have already been obtained by complexation of $[Re_6S^i_8(CN)^a_6]^{3-}$ and $[Re_6S^i_8(CN)^a_6]^{4-}$ with Ga^{3+} to form $Ga[Re_6S^i_8(CN)^a_6]\text{-}6H_2O$ and $Ga_4[Re_6S^i_8(CN)^a_6]_3\text{-}38H_2O$, respectively. Such structures, built up from cluster units, exhibit a high porosity with voids of 42% and 56%, respectively. These voids can be generated because of a cubic neutral framework resulting from the charge balance between $[Re_6S^i_8(CN)^a_6]^{3-}$ or $[Re_6S^i_8(CN)^a_6]^{4-}$ cluster

units and Ga^{3+}.[31] Hitherto and despite many efforts, single crystals of molybdenum homologous with '$M[Mo_6Br^i_8(CN)^a_6]\cdot xH_2O$' analogous with ferri–ferricyanide have not yet been obtained. On the other hand, $[trans\text{-}Cd(H_2O)_2][Mo_6Br^i_8(CN)^a_6]$ was successfully obtained as single crystals. The structure of $[trans\text{-}Cd(H_2O)_2][Mo_6Br^i_8(CN)^a_6]$ is strongly related to that of $Cs_2[trans\text{-}M(H_2O)_2][Re_6S^i_8(CN)^a_6]$ (M = Fe, Mn, Zn and Cd).[23] Indeed both structures are based on layers built up from cluster units and $trans\text{-}[M(H_2O)_2]^{2+}$ complexes. This enables the formation of a square-net-layers of alternating $[trans\text{-}M(H_2O)]^{2+}$ cations and anionic clusters units. The anionic charge of the $\{[trans\text{-}M(H_2O)_2][Re_6S^i_8(CN)^a_6]\}^{2-}$ layer is compensated by the presence of Cs^+ cations. Half of cesium atoms lie in half of the voids within this layer. The other half of cesium atoms are located between the layers. Owing to the lower charge of the $[Mo_6Br^i_8(CN)^a_6]^{2-}$ cluster units compared to the $[Re_6S^i_8(CN)^a_6]^{4-}$ one and consequently owing to the absence of alkali earth ions, the $[trans\text{-}Cd(H_2O)_2][Mo_6Br^i_8(CN)^a_6]$ structure contains 15% of voids. An interesting finding is the formation of hollow tubular channels with an aperture of about 1.30 Å and cavities of about 80 $Å^3$. Similarly to the description of the structure of $Cs_2[trans\text{-}M(H_2O)_2][Re_6S^i_8(CN)^a_6]$, $[trans\text{-}Cd(H_2O)_2][Mo_6Br^i_8(CN)^a_6]$ can be depicted as 2D extended polymeric square-net-layers formed by the connection *via* ionic interactions of $[trans\text{-}Cd(H_2O)_2]^{2+}$ with four $[Mo_6Br^i_8(CN)^a_6]^{2-}$ cluster units in the (*a*,*c*) plane. These square-net-layers fit together along the *b* direction. The channels are parallel to the *a* axis and centred on the (0, 1/2, 1/2) position (Fig. 1).

However, it is worth noting that there exists a strong close packing of the cluster cores in the (*a*,*b*) plane. Indeed the $Br1^i$–$Br1^i$ inter-units distances correspond to the sum of van der Waals radii (ESI†). Thus, the structure can be depicted as a close packing of cluster units in the (*a*,*b*) plane forming a distorted hexagonal lattice. Each cluster unit is surrounded by four cluster units with short distances of 8.7013(2) Å and by two other cluster units at longer distances of 10.6047(3) Å. A pseudo-hexagonal cell can be drawn with a_h = 8.7013(2) Å, c_h = 9.8525(3) Å, and γ_h = 104.91°. This pseudo-hexagonal cell characterized by a AA′A stacking of units is represented in Fig. 2. Such staking generates prismatic sites of units wherein lie the $[trans\text{-}Cd(H_2O)_2]^{2+}$ complexes in one half of the prismatic sites. Let us stress that such type of stacking and environments is closely related to those found earlier in the $M(RE)M_6X_{18}$ series.[32] Beyond ionic interactions between $[trans\text{-}Cd(H_2O)_2]^{2+}$ complexes and $[Mo_6Br^i_8(CN)^a_6]^{2-}$ cluster units, the cohesion of the structure is ensured by $Br1^i$–$Br1^i$ van der Waals interactions, hydrogen bonding between water molecules and bromines (O2w-Br3 3.663(8) (×2); O2w-Br3: 3.661(2) Å) and between C1N1 and water molecules (N1–O1w = 2.738 (9) Å). Note that, the splitting of the O_2 oxygen of the second water molecule coordinated to Cd^{2+} on two close positions is easily explained by the weakness of the hydrogen bonding between this water molecules and Br3 that is larger by 0.2 Å than those reported in some related hydrated cadmium or cobalt bromide complexes.[33]

3.3. Synthesis of promesogenic ammonium salt and corresponding hybrids

As reported previously, the radius of the cluster anion $[Re_6Se_8(CN)_6]^{n-}$ defined as the distance from the centre of the cluster nucleus to the N atom including van der Waals radii is 6.65 Å.[34] A very similar value of 6.77 Å could be deduced for $[Mo_6Br_8(CN)_6]^{2-}$ from the structural data of $[trans\text{-}Cd(H_2O)_2][Mo_6Br^i_8(CN)^a_6]$. Therefore, we can state that the same volume is occupied by inorganic entities in our LC material whatever the nature of the metal and the ligands building the $M_6L^i_8$ cluster core. In order to design a suitable cation that should, *a priori*, induce mesomorphism, we made the hypothesis that the cross section of the inorganic part of the material should be at least compensated by the one of its organic counterpart. Therefore, some simple geometrical

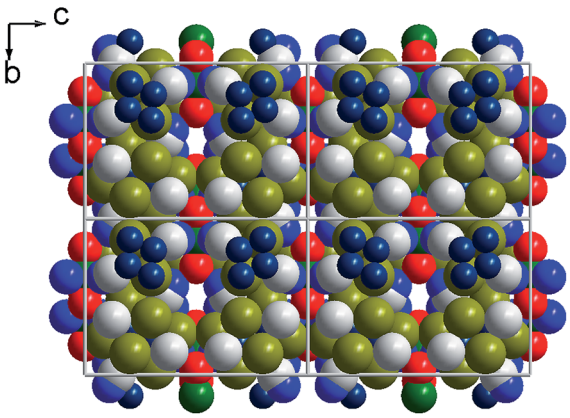

Fig. 1 Space filling model of the projection of the crystal structure of $[trans\text{-}Cd(H_2O)_2][Mo_6Br^i_8(CN)^a_6]$ in the (*b*,*c*) plane evidencing the channels parallel to the *a* axis centred on 0, 1/2, 1/2 with cavities of 83 $Å^3$ and aperture of 1.33 Å. Dark yellow: Br; dark blue: Mo; blue: N; red: O; light grey: C; green: Cd.

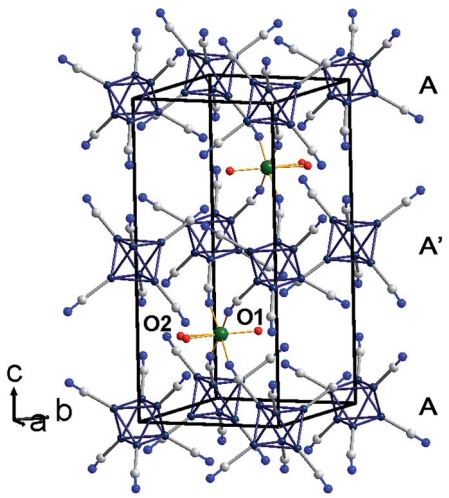

Fig. 2 Representation of the pseudo-hexagonal lattice with the AA′A packing evidencing the cluster unit prismatic environment of $[trans\text{-}Cd(H_2O)_2]$. For sake of clarity, inner ligands are not represented. The unit of the A′ layer correspond to that of the A layer by a mirror plane operation. The *a*,*b*,*c* coordinated system is that of the orthorhombic unit cell. Dark blue: Mo; blue: N; red: O; light grey: C; green: Cd.

statements can be made to design the optimal organic cation: (i) the cross section surface of one cluster is close to 140 Å^2; (ii) the transverse cross section of one CB unit is about 22 to 25 Å^2. Therefore, 6 CB units should be required to compensate the cross section of one cluster. Indeed, using the earlier described two CB units containing ammonium cation[20] with $[Mo_6Br_8(CN)_6]^{2-}$ did not lead to mesomorphic material. We therefore synthesized a new functional ammonium bearing three decyloxy chains terminated by CB units as depicted in Fig. 3. This cation was obtained pure after column chromatography as a bromide salt, by reaction of three equivalents of 4′-(10-bromodecyloxy)-4-cyanobiphenyl with methylamine in ethanol (see Experimental part for further details) and was fully characterized by usual techniques. The hybrid materials were then obtained by cationic metathesis replacing the alkali counter-cations of the cluster precursors by the mesogenic ammonium salts. The desired products precipitated immediately when an ethanol solution of the organic salts was added to a solution of clusters. The products were purified by washing with hot water and hot ethanol. The purity of the compounds was confirmed by EDS with lack of bromine in the case of **3** and **4** and the absence cluster inorganic counter cation (cesium or potassium, depending on the cluster), ^{1}H NMR, ^{13}C NMR and elemental analysis.

3.4. Self-organization properties

The liquid crystal behaviour of our new compounds were first investigated by polarized optical microscopy (POM) and differential scanning calorimetry (DSC). All samples underwent three heating/cooling cycles from −20 °C up to 200 °C to record DSC thermograms (Table 1 gathers results from the second heating cycle). For all compounds, DSC thermograms show at high temperature broad LC to isotropic state transitions either on heating or cooling cycles and, at low temperature, a glass transition corresponding to the freezing of the mesophase (see ESI† for thermograms). Depending on the compound's thermal history, the first heating cycle may reflect the usual complicated thermal behaviour of supermolecular systems with several endo or exothermic signals.[35] For **1**, **2** and **4** all heating (except the first one) and cooling cycles are superimposable meaning that compounds are thermally stable.

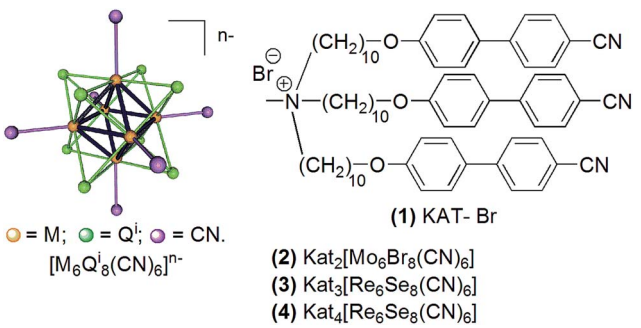

Fig. 3 Schematic representation of hybrid compounds synthesized in this work.

Table 1 Thermal transitions observed for compounds **1** to **4**

Compound	Transition	T/°C[a]	ΔH[a]/kJ mol^{-1}
1	I–N	113	5
	N-SmA	103[b]	
	SmA-G	35	
2	I–N	97[b]	5.6
	N-SmA	90[b]	
	SmA-G	47	
3	I-SmA	112	5.5
	SmA-G	44	
4	I-SmA	124	15.6
	SmA-G	26	

[a] Data from the second heating cycle. [b] Temperature observed on cooling by POM.

For compound **3**, a slight evolution in the position of the transition maximum signals was observed when the sample was heated up to 200 °C and is correlated to the reduction of some $[Re_6Se_8(CN)_6]^{3-}$ into $[Re_6Se_8(CN)_6]^{4-}$ (*vide infra*). Heating the sample only up to 130 °C gave superimposable DSC thermograms (see ESI, Fig. S9†) attesting its stability at lower temperature. In all cases, the thermograms of **2**, **3** and **4** do not show the transitions observed for **1** which indicates that there is no excess of **1** in the materials. The organic salt **1** presents a nematic phase at 113 °C, which is converted into a smectic phase on cooling to 103 °C. This transition is clearly seen by POM although the DSC showed only one broad transition at 113 °C. On further cooling the compound passes to a glassy state. The three compounds, **2**, **3** and **4**, with 6, 9 and 12 mesogenic units, respectively, presented liquid crystal behaviour. For all three a glassy state was observed, by DSC, at 52 °C for compound **2** and it decreased to 36 °C and 26 °C for Re based hybrid (**3** and **4**, respectively). The mesophases were investigated by POM and the textures are presented in Fig. 4.

For compound **2**, which contains 6 mesogenic units around the cluster, a schlieren texture on heating and cooling cycles was observed. This texture was homogeneous and characteristic of a nematic phase (Fig. 4a). On cooling to 90 °C the nematic phase passed to a lamellar smectic phase (Fig. 4b). The transition from nematic to smectic phase could not be detected by DSC as the signal was very broad even when the heating or cooling rate was reduced to 1 K min^{-1}. For compound **3**, with 9 mesogenic units around the cluster, and compound **4** bearing 12 mesogenic units, typical focal conic fan textures characteristic of layered phases were observed. In order to assign the exact nature of the liquid crystalline phases, the compounds were also characterized by small angle X-ray diffraction. As clearing temperatures are much below thermal decomposition temperature, compounds could be heated until their isotropic state and slowly cooled down to reach the desired mesophase. For **2**, a first diffractogram that was recorded at 95 °C contains broad and intense signals centred at 1.9 and 3.8 nm^{-1} corresponding to lengths of 33.1 Å and 16.2 Å respectively, and interpreted as the intermolecular short-range interactions that are parallel and perpendicular to the molecular long axis, respectively. This diffractogram was assigned to a nematic

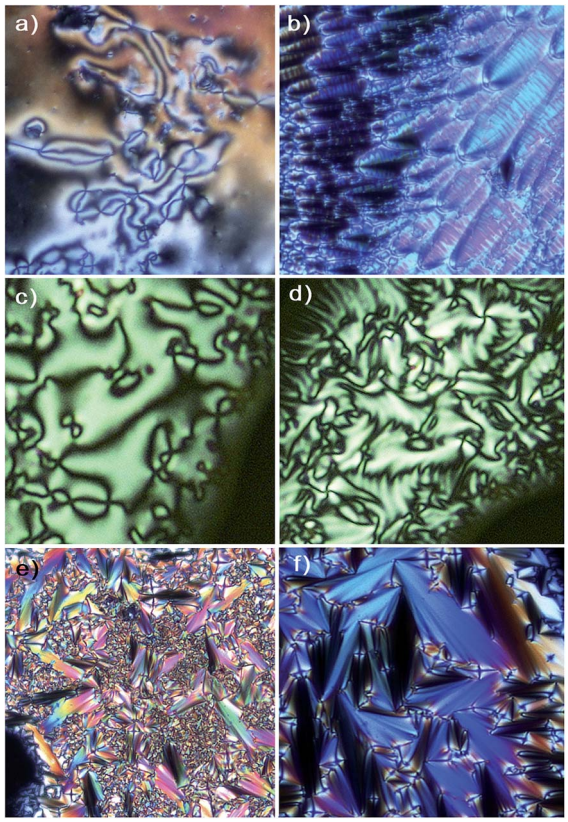

Fig. 4 Polarized optical micrographs of (a) compound **1** in the nematic phase at 120 °C (temperature of the heating stage). (b) Compound **1** in the smectic phase at 50 °C. (c) Compound **2** in the nematic phase at 96 °C. (d) Compound **2** in the smectic phase at 86 °C. (e) Compound **3** in the smectic phase at 100 °C and (f) compound **4** in the smectic phase at 110 °C.

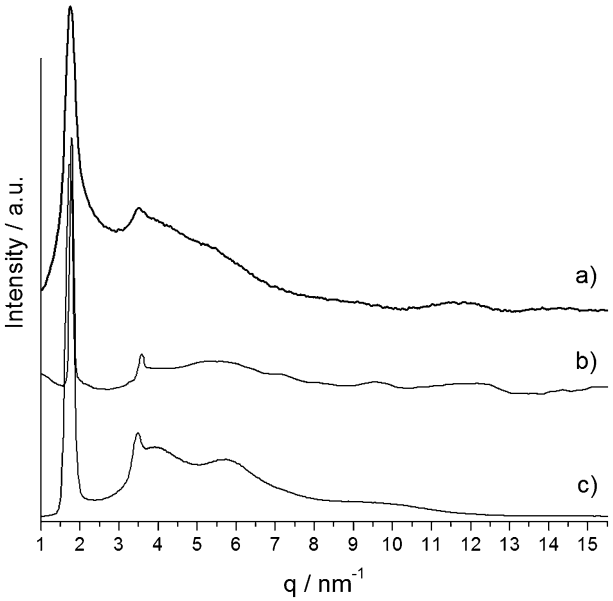

Fig. 5 Temperature dependent X-ray diffractograms taken at (a) 70 °C for **2**, (b) 90 °C for **3**, and (c) 90 °C for **4**.

phase (see ESI†). Lowering the temperature induces the formation of two relatively sharp signals (explanations on the width of those signals are given below) with a reciprocal spacing in the 1 : 2 ratio that correspond to a lamellar organization with an interlayer spacing of 36 Å (Fig. 5).

The nematic to smectic transition was not observed by DSC although a close examination of the thermograms shows a combined peak with a shoulder (ESI†). Temperature dependent diffractograms of compounds **3** and **4** are similar: two sharp reflexions in the low angle region indicative of a long range order. For compound **3**, these two diffraction peaks in the ratio 1 : 2 correspond to a lamellar organization with an interlayer distance of 35.2 Å at 95 °C, in accordance with the SmA texture presented by POM. On further cooling the phase is maintained. In the case of **4**, the two sharp reflections in the ratio 1 : 2 correspond also to a lamellar organization with a periodicity of 36 Å ($d = d_{001} = 36.1$ Å, $d_{002} = 18$ Å).

Therefore, we observe that in the three compounds the interlayer distance is very similar. Note also that a close value was calculated for equivalent compounds with a bisubstituted ammonium (an interlayer spacing distance of 37.4 Å was obtained).[20] This point was expected and in good accordance with previous results obtained with commercial alkyl ammonium cations and rhenium clusters. Indeed, Suh *et al.* demonstrated that the interlayer distance value is governed in this case by the length of the ammonium alkyl chains.[36] Therefore, if the rod-like molecular shape of hybrids does not vary significantly in height, it should increase in width together with the cluster charge so as to accommodate the molecular volume of the supplementary organic cations. According to molecular models (Fig. 6), an interspacing distance of 36 Å may imply a full interdigitation of CB moieties

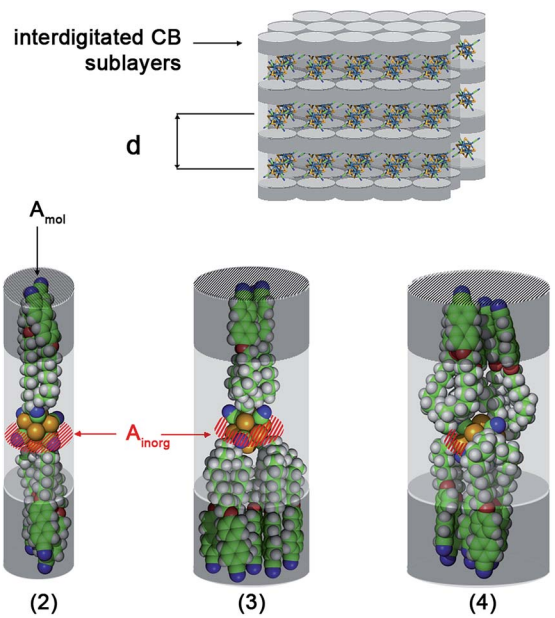

Fig. 6 Representation of the different molecular hybrids and their organization into layers at low temperature.

which corresponds to surfaces of 6, 9 or 12 CB units per layer and per cluster for **2**, **3** and **4**, respectively (assuming that CB are equally distributed on both cluster sides).

Note that the case of **3** is different as an odd number of CB is present in the compound. In this case, we assume that the lack of CB on one side of the cluster is compensated by a cluster from an adjacent layer. This should affect the organization of clusters within the layers and therefore can reasonably be considered as a factor that induces the smectic A character of the observed mesophase. This point is corroborated by a closer observation of X-ray diffractograms: layered phases containing hybrids with an even number of cations (and thus even number of mesogenic units), namely **2** and **4** seem more ordered. Indeed, diffractograms presented in Fig. 5 show additional broad and intense reflexions related to the short range in plane ordering of clusters within the layers that are particularly intense for **2** and **4**. These signals are also much larger in case of **2** than for **4** meaning that the layered phase of **4** is more ordered. The diffractogram for compound **3** lacks these reflexions probably because of its odd number of mesogens which implies a more disordered cluster arrangement within the inorganic planes. In the case of **2** we see that the surface occupied by the mesogens barely compensate the surface of the inorganic counterpart (A_{inorg} in Fig. 6). As a result, cluster anions should be closer one to another, enhancing anion–anion coulombic repulsion that could explain (i) the appearance of the nematic phase between 90 °C and 97 °C, (ii) the much larger width of compound **2** d_{001} signal as compared to compounds **3** and **4**. Indeed, an increased mobility of the organic chains should enhance this coulombic repulsion phenomena avoiding clusters to lay close to each other and *a fortiori* in the same plane. Lowering the temperature would be more profitable for the organic/inorganic segregation phenomenon that would take the lead on the self-assembling process. For **4**, a completely different phenomenon occurs, as the transverse cross section of clusters is largely compensated by the one of the twelve CB units located on each of its sides. In this specific case, the molecular self-assembling process is mainly driven by the usual dipole–dipole organic–organic interactions found in the self-assembling process of organic liquid crystal materials. It leads to a better structuration of the material and thus more defined signals. However, although the X-ray diffractogram of **4** corresponds to a more structured system, the broadness of signals precludes any clear interpretation of the clusters local ordering within the layers (hexagonal *vs.* square arrangement). The first large signal position at smaller angle corresponding to the lateral cluster ordering is located at 3.9 nm^{-1}, which corresponds to a distance of 16.1 Å between the clusters scattering planes. One could eventually argue that this value seems in good accordance with a hexagonal arrangement of clusters within the layers as related calculations would give, in this case, a transverse cross-section value of 22.6 $Å^2$ per CB unit, a value in good agreement with previously reported value for such cross-section.

3.5. Physico-chemical properties of hybrids

Compounds **2** and **4** are luminescent in the red-NIR while compound **3** is not but shows magnetic properties. The paramagnetic character of **3** was demonstrated by EPR measurements realized at 77 K (ESI†). The calculated g value ($g = 2.55$) is identical to the one we reported[20] for a similar compound and is in the range of previously reported ones for hexanuclear rhenium cluster anions ($[Re_6Q_8L_6]^{3-}$ (Q = S, Se, Te; L = CN, Cl, Br; 2.44–2.56)). The magnetic moment $\mu_{eff} = 2.2\ \mu_B$ of **3** is larger than the spin 1/2-only value ($\mu_{SO} = 1.73\ \mu_B$), which is in agreement with a high spin–orbit coupling.[37]

Absorption studies were realized in solution (ESI†) while photoluminescence measurements of **2** and **4** were performed in their LC and glass phases. This is the first time that luminescence properties of the $[Mo_6Br^i_8(CN)^a_6]^{2-}$ cluster anion are reported. Fig. 7 presents excitation and emission spectra obtained for both compounds at 20 °C. We observe the usual behaviour of luminescent octahedral clusters containing either molybdenum or rhenium atoms: a large excitation window going from UV to 550–600 nm and a large emission window in the red-NIR area with a large Stokes-shift. Increasing temperature induces a decrease of the signal intensity. Compound **4** was deposited on a microscope quartz slide and its emission *vs.* temperature was studied by using a polarized microscope equipped with a hot stage, an irradiation source and a CCD photodetector. Spectra were recorded on cooling from the isotropic state at 413 K to 313 K (Fig. 8).

Lowering the temperature induces an increase of the emission intensity due to less non radiative deactivation of the excited state and therefore, the emission intensity is expected to increase following an exponential law of the type $I(T) = I_0 \exp(-A/T)$ where A is a constant and I_0 the emission intensity at a given temperature (in our case: 313 K).[6,38] According to this equation, reporting $\ln(I/I_{313})$ *versus* the inverse of absolute temperature (inset Fig. 8) should give a straight line if no other parameters were involved in the emissive process.

It is clear from Fig. 8 that the phase transition from isotropic to LC (starting at 124 °C and finishing around 100 °C from DSC measurements) affects strongly the luminescence intensity as the plot can be divided in two parts with an edge corresponding

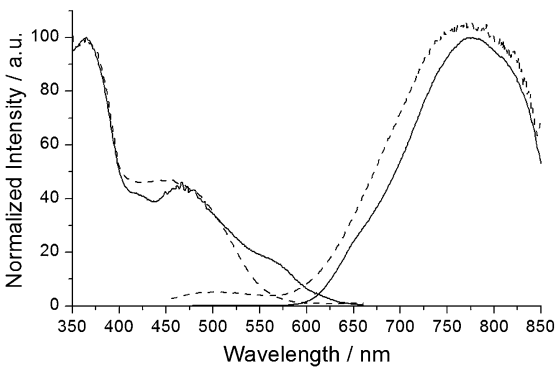

Fig. 7 Excitation (λ_{obs} = 680 nm, left) and emission (λ_{exc} = 435 nm, right) spectra of compounds **2** (dashed line) and **4** (plain line) at 20 °C.

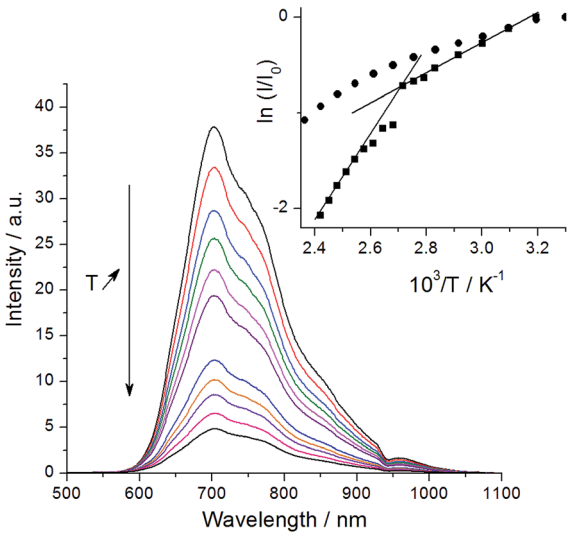

Fig. 8 Temperature dependent emission spectra (λ_{exc} = 400 nm) of compound **4**. Inset: evolution of signal intensity at 705 nm in function of temperature for **4** (squares) and $KCs_3Re_6Se_8(CN)_6$ (circles).

to this transition (such phenomenon is not observed for the clustomesogen precursor $KCs_3Re_6Se_8(CN)_6$ as depicted by the inset in Fig. 8). Therefore, it shows that, despite the isotropy of the emissive species, the molecular orientation and by extension the nanostructuration of the material into layers modify the ability of the material to emit light. In our previous studies, we showed that the nature of the organic counter cation of $[Re_6Se_8CN_6]^{n-}$ with $n = 3$ or 4 does not influence their intrinsic behaviour within the hybrid materials.[20] Therefore, compound **3** is not supposed to show luminescence properties as only diamagnetic clusters with 24 electrons in their VEC behave so, and, as expected, a flat signal, even with very long integration time, was recorded at 20 °C (Fig. 9, dashed line curve) when the sample was irradiated between two quartz slides. It is clear from this measurement that **3** is not luminescent. However, irradiation after a thermal treatment consisting of heating the sample

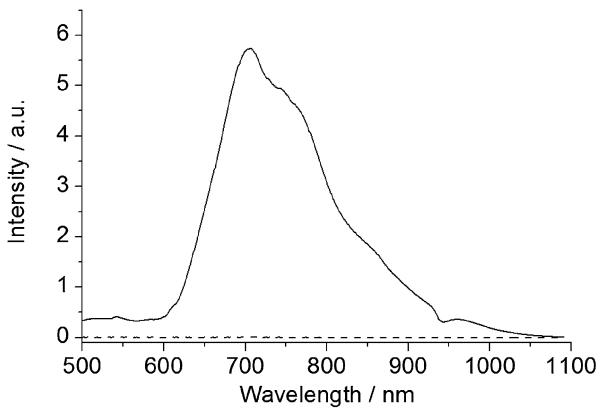

Fig. 9 Luminescence spectra of **3** before (dashed line, integration time 30 s) and after (plain line, integration time 10 s) heating at 150 °C for 30 min.

at 150 °C for 30 min and cooling it back to 20 °C, induces the appearance of a luminescence signal similar to the one of **4**.

As the oxidation of $[Re_6Se_8(CN)_6]^{4-}$ is reversible and occurs at low potential ($E^{0'}$ = 0.27 *vs.* SCE), it is possible that little amount of $[Re_6Se_8(CN)_6]^{3-}$ may have been reduced at high temperature and thus leads to the formation of luminescent material. It has to be noted that no significant change in the colour of the material could be detected (going from dark green to orange). Therefore we suspect that only a small amount of **3** could be converted into **4** after several heating and cooling cycles and this assumption is in good accordance with results obtained by DSC when **3** is heated above 130 °C.

4. Conclusions

We show in this work (i) the versatility of the $[Mo_6Br_8(CN)_6]^{2-}$ cluster unit for the design of new materials and (ii) that it is possible to tailor the mesomorphic behaviour from nematic to smectic of ionically self-assembled clustomesogen by modifying the ratio between the organic and inorganic content in the $(Kat)_n[M_6Y^i_8(CN)^a_6]$ LC materials using hexacyano $[M_6Y^i_8(CN)^a_6]^{n-}$ ($n = 2$ and M = Mo, Y = Br; $n = 3$, 4 and M = Re, Y = Se) cluster building blocks. To do so, we implemented a new and efficient high yield synthesis route for the $[Mo_6Br_8(CN)_6]^2$ inorganic building block. Interestingly, we showed that it is highly stable in water and thus that it could be involved in the preparation of the $[trans\text{-}Cd(H_2O)_2][Mo_6Br^i_8(CN)^a_6]$ extended polymeric framework that was characterized by single crystal X-ray diffraction. The latter can be viewed as the first member of extended polymeric frameworks based on Mo_6 clusters. Structural correlations between $[trans\text{-}Cd(H_2O)_2][Mo_6Br^i_8(CN)^a_6]$ with related extended polymeric frameworks based on $[Re_6S^i_8(CN)^a_6]^{3-}$ or $[Re_6S^i_8(CN)^a_6]^{4-}$ have been evidenced. Indeed, this work will be pushed forward in order to obtain Mo_6 cluster-based frameworks porosity as high as those reported for Re_6 cluster based ones and to associate such structural properties with for instance photo-catalytic properties of Mo_6 clusters.[13] Moreover, $[Mo_6Br_8(CN)_6]^{2-}$ cluster unit is a relevant building block for the synthesis of new hybrid LC material containing mesomorphic ammonium cations. Following the same procedure as the one used for $[Mo_6Br_8(CN)_6]^{2-}$, we obtained similar hybrid materials containing $[Re_6Se_8(CN)_6]^{3-}$ or $[Re_6Se_8(CN)_6]^{4-}$. These three transition metal cluster units, having the same face-capped geometry and consequently the same volume but bearing different charges, were used to tailor the organic entities/inorganic entities volume ratio within $(Kat)_n[M_6Y^i_8(CN)^a_6]$ hybrid material (n = 2, 3 and 4) and therefore the organic part transverse cross section area. At low organic/inorganic ratio, nematogenic behaviour is promoted because of the enhancement of coulombic interactions between anionic clusters that is favoured by the mobility of the organic chains at high temperature. Lowering the temperature induces a behaviour in which phase segregation is predominant and as a result, successive inorganic and organic layers are observed. For higher organic content, self-assembling processes are directed by the dipole–dipole interactions between CB units and only layered phases are observed on a broad temperature range

from 26 °C to 124 °C. As expected, clusters retain their intrinsic properties (bright red NIR luminescence for compounds **2** and **4** and magnetism for **3**) in the hybrid material even though some reduction of $[Re_6Se_8(CN)_6]^{3-}$ in $[Re_6Se_8(CN)_6]^{4-}$ has been evidenced upon heating at 150 °C. We could also evidence, for the first time in the clustomesogen family, that the material nanostructuration was influencing its ability to emit light despite the isotropy of the emissive species and therefore temperature dependent photoluminescence measurements could be also used to determine phase transition temperature. Finally, among the $(Kat)_n[M_6Y^i{}_8(CN)^a{}_6]$ family, $(Kat)_2Mo_6Br^i{}_8(CN)^a{}_6$ is the only one that exhibit a nematic behaviour, the least ordered and most fluid LC phase, which is particularly rare for ionic compounds and of peculiar interest for the development of LC based devices needing stable red emitters.

Acknowledgements

The authors thank T. Guizouarn for EPR, and Dr V. Marchi Artzner for access to the spectrofluorimeter. We thank the France-Russia programs PICS (2011–2013 no. 5822) and International Associate Laboratory (2014–2017) as well as the IDEMAT chemistry project in the frame of the Franco Siberian Center of Training and Research. This work was funded by Fondation Langlois, Région Bretagne and ANR Clustomesogen ANR-13-BS07-0003-01.

Notes and references

1 C. Sanchez, K. J. Shea and S. Kitagawa, *Chem. Soc. Rev.*, 2011, **40**, 471; C. Sanchez, P. Belleville, M. Popall and L. Nicole, *Chem. Soc. Rev.*, 2011, **40**, 696.

2 D. W. Bruce, D. A. Dunmur, E. Lalinde, P. M. Maitlis and P. Styring, *Nature*, 1986, **323**, 791; A. M. Giroud-Godquin and P. M. Maitlis, *Angew. Chem., Int. Ed.*, 1991, **30**, 375; B. Donnio, D. Guillon, R. Deschenaux and D. W. Bruce, in *Comprehensive Coordination Chemistry II: From Biology to Nanotechnology*, ed. J. A. Mc Cleverty, J. J. Meyer, M. Fujita and A. Powell, Elsevier, Oxford, 2003, p. 357; K. Binnemans, *J. Mater. Chem.*, 2009, **19**, 448.

3 J. R. Long, L. S. McCarty and R. H. Holm, *J. Am. Chem. Soc.*, 1996, **118**, 4603; K. Kirakci, S. Cordier and C. Perrin, *Z. Anorg. Allg. Chem.*, 2005, **631**, 411.

4 S. Cordier, Y. Molard, K. A. Brylev, Y. V. Mironov, F. Grasset, B. Fabre and N. G. Naumov, *J. Cluster Sci.*, 2014, DOI: 10.1007/s10876.

5 T. G. Gray, C. M. Rudzinski, E. E. Meyer, R. H. Holm and D. G. Nocera, *J. Am. Chem. Soc.*, 2003, **125**, 4755; T. G. Gray, C. M. Rudzinski, D. G. Nocera and R. H. Holm, *Inorg. Chem.*, 1999, **38**, 5932; A. W. Maverick, J. S. Najdzionek, D. MacKenzie, D. G. Nocera and H. B. Gray, *J. Am. Chem. Soc.*, 1983, **105**, 1878.

6 N. Kitamura, Y. Ueda, S. Ishizaka, K. Yamada, M. Aniya and Y. Sasaki, *Inorg. Chem.*, 2005, **44**, 6308.

7 M. N. Sokolov, M. A. Mihailov, E. V. Peresypkina, K. A. Brylev, N. Kitamura and V. P. Fedin, *Dalton Trans.*, 2011, **40**, 6375; A. W. Maverick and H. B. Gray, *J. Am. Chem. Soc.*, 1981, **103**, 1298.

8 F. A. Cotton, *Inorg. Chem.*, 1964, **3**, 1217.

9 S. Cordier, K. Kirakci, D. Mery, C. Perrin and D. Astruc, *Inorg. Chim. Acta*, 2006, **359**, 1705.

10 J. R. Long, L. S. McCarty and R. H. Holm, *J. Am. Chem. Soc.*, 1996, **118**, 4603.

11 S. Ababou-Girard, S. Cordier, B. Fabre, Y. Molard and C. Perrin, *ChemPhysChem*, 2007, **8**, 2086; F. Grasset, Y. Molard, S. Cordier, F. Dorson, M. Mortier, C. Perrin, M. Guilloux-Viry, T. Sasaki and H. Haneda, *Adv. Mater.*, 2008, **20**, 1710; F. Grasset, F. Dorson, Y. Molard, S. Cordier, V. Demange, C. Perrin, V. Marchi-Artzner and H. Haneda, *Chem. Commun.*, 2008, 4729; F. Grasset, F. Dorson, S. Cordier, Y. Molard, C. Perrin, A.-M. Marie, T. Sasaki, H. Haneda, Y. Bando and M. Mortier, *Adv. Mater.*, 2008, **20**, 143; A. Garreau, F. Massuyeau, S. Cordier, Y. Molard, E. Gautron, P. Bertoncini, E. Faulques, J. Wery, B. Humbert, A. Bulou and J. L. Duvail, *ACS Nano*, 2013, **7**, 2977; T. Aubert, F. Cabello-Hurtado, M. A. Esnault, C. Neaime, D. Lebret-Chauvel, S. Jeanne, P. Pellen, C. Roiland, L. Le Polles, N. Saito, K. Kimoto, H. Haneda, N. Ohashi, F. Grasset and S. Cordier, *J. Phys. Chem. C*, 2013, **117**, 20154; S. Cordier, B. Fabre, Y. Molard, A. B. Fadjie-Djomkam, N. Tournerie, A. Ledneva, N. G. Naumov, A. Moreac, P. Turban, S. Tricot, S. Ababou-Girard and C. Godet, *J. Phys. Chem. C*, 2010, **114**, 18622.

12 H. D. Selby, B. K. Roland and Z. Zheng, *Acc. Chem. Res.*, 2003, **36**, 933.

13 D. Mery, L. Plault, S. Nlate, D. Astruc, S. Cordier, K. Kirakci and C. Perrin, *Z. Anorg. Allg. Chem.*, 2005, **631**, 2746; D. Mery, L. Plault, C. Ornelas, J. Ruiz, S. Nlate, D. Astruc, J. C. Blais, J. Rodrigues, S. Cordier, K. Kirakci and C. Perrin, *Inorg. Chem.*, 2006, **45**, 1156; L. F. Szczepura, K. A. Ketcham, B. A. Ooro, J. A. Edwards, J. N. Templeton, D. L. Cedeno and A. J. Jircitano, *Inorg. Chem.*, 2008, **47**, 7271; G. Prabusankar, Y. Molard, S. Cordier, S. Golhen, Y. Le Gal, C. Perrin, L. Ouahab, S. Kahlal and J. F. Halet, *Eur. J. Inorg. Chem.*, 2009, 2153; Y. Molard, F. Dorson, K. A. Brylev, M. A. Shestopalov, Y. Le Gal, S. Cordier, Y. V. Mironov, N. Kitamura and C. Perrin, *Chem.–Eur. J.*, 2010, **16**, 5613.

14 C. Echeverria, A. Becerra, F. Nunez-Villena, A. Munoz-Castro, J. Stehberg, Z. Zheng, R. Arratia-Perez, F. Simon and R. Ramirez-Tagle, *New J. Chem.*, 2012, **36**, 927.

15 M. Amela-Cortes, A. Garreau, S. Cordier, E. Faulques, J.-L. Duvail and Y. Molard, *J. Mater. Chem. C*, 2014, **2**, 1545; Y. Molard, C. Labbe, J. Cardin and S. Cordier, *Adv. Funct. Mater.*, 2013, **23**, 4821.

16 A. Barras, M. R. Das, R. R. Devarapalli, M. V. Shelke, S. Cordier, S. Szunerits and R. Boukherroub, *Appl. Catal., B*, 2013, **130–131**, 270; A. Barras, S. Cordier and R. Boukherroub, *Appl. Catal., B*, 2012, **123–124**, 1; P. Kumar, S. Kumar, S. Cordier, S. Paofai, R. Boukherroub and S. L. Jain, *RSC Advances*, 2014, **4**, 10420.

17 Y. Zhao and R. R. Lunt, *Adv. Energy Mater.*, 2013, **3**, 1143.

18 T. Yoshimura, S. Ishizaka, Y. Sasaki, H. B. Kim, N. Kitamura, N. G. Naumov, M. N. Sokolov and V. E. Fedorov, *Chem. Lett.*, 1999, 1121.
19 C. F. J. Faul and M. Antonietti, *Adv. Mater.*, 2003, **15**, 673.
20 Y. Molard, A. Ledneva, M. Amela-Cortes, V. Circu, N. G. Naumov, C. Meriadec, F. Artzner and S. Cordier, *Chem. Mater.*, 2011, **23**, 5122.
21 A. S. Mocanu, M. Amela-Cortes, Y. Molard, V. Circu and S. Cordier, *Chem. Commun.*, 2011, **47**, 2056; M. Amela-Cortes, F. Dorson, M. Prévôt, A. Ghoufi, B. Fontaine, F. Goujon, R. Gautier, V. Cîrcu, C. Mériadec, F. Artzner, H. Folliot, S. Cordier and Y. Molard, *Chem.–Eur. J.*, 2014, **20**, 8561.
22 Y. Molard, F. Dorson, V. Circu, T. Roisnel, F. Artzner and S. Cordier, *Angew. Chem., Int. Ed.*, 2010, **49**, 3351.
23 L. G. Beauvais, M. P. Shores and J. R. Long, *Chem. Mater.*, 1998, **10**, 3783.
24 M. Roessle, E. Manakova, I. Lauer, T. Nawroth, J. Holzinger, T. Narayanan, S. Bernstorff, H. Amenitsch and H. Heuman, *J. Appl. Crystallogr.*, 2000, **33**, 548.
25 Y. V. Mironov, J. A. Cody, T. E. AlbrechtSchmitt and J. A. Ibers, *J. Am. Chem. Soc.*, 1997, **119**, 493.
26 Z. Zheng, J. R. Long and R. H. Holm, *J. Am. Chem. Soc.*, 1997, **119**, 2163; A. Y. Ledneva, K. A. Brylev, A. I. Smolentsev, Y. V. Mironov, Y. Molard, S. Cordier, N. Kitamura and N. G. Naumov, *Polyhedron*, 2014, **67**, 351.
27 M. K. Simsek, D. Bublitz and W. Preetz, *Z. Anorg. Allg. Chem.*, 1997, **623**, 1885.
28 N. G. Naumov, S. Cordier and C. Perrin, *Angew. Chem., Int. Ed.*, 2002, **41**, 3002; N. G. Naumov, S. Cordier and C. Perrin, *Solid State Sci.*, 2003, **5**, 1359; S. Cordier, N. G. Naumov, D. Salloum, F. Paul and C. Perrin, *Inorg. Chem.*, 2004, **43**, 219; N. G. Naumov, S. Cordier and C. Perrin, *Solid State Sci.*, 2005, **7**, 1517.
29 H. J. Zhou and A. Lachgar, *Eur. J. Inorg. Chem.*, 2007, 1053; J. J. Zhang and A. Lachgar, *J. Am. Chem. Soc.*, 2007, **129**, 250; H. Zhou and A. Lachgar, *Cryst. Growth Des.*, 2006, **6**, 2384.
30 M. V. Bennett, M. P. Shores, L. G. Beauvais and J. R. Long, *J. Am. Chem. Soc.*, 2000, **122**, 6664; N. G. Naumov, A. V. Virovets, M. N. Sokolov, S. B. Artemkina and V. E. Fedorov, *Angew. Chem., Int. Ed.*, 1998, **37**, 1943; N. G. Naumov, D. V. Soldatov, J. A. Ripmeester, S. B. Artemkina and V. E. Fedorov, *Chem. Commun.*, 2001, 571.
31 M. V. Bennett, L. G. Beauvais, M. P. Shores and J. R. Long, *J. Am. Chem. Soc.*, 2001, **123**, 8022.
32 S. Cordier, C. Perrin and M. Sergent, *J. Solid State Chem.*, 1995, **118**, 274; S. Cordier, C. Perrin and M. Sergent, *Z. Anorg. Allg. Chem.*, 1993, **619**, 621.
33 A. C. Blackburn, J. C. Gallucci and R. E. Gerkin, *Acta Crystallogr., Sect. C: Cryst. Struct. Commun.*, 1991, **47**, 282; K. Slepokura and T. Lis, *Acta Crystallogr., Sect. C: Cryst. Struct. Commun.*, 2008, **64**, M127.
34 N. G. Naumov, A. V. Virovets, N. V. Podberezskaya and V. E. Fedorov, *J. Struct. Chem.*, 1997, **38**, 857.
35 E. Terazzi, G. Rogez, J.-L. Gallani and B. Donnio, *J. Am. Chem. Soc.*, 2013, **135**, 2708; C. Tschierske, Liquid Crystals: Materials Design and Self-Assembly, in *Top. Curr. Chem.*, 2012, vol. 318, 2012; E. Terazzi, C. Bourgogne, R. Welter, J.-L. Gallani, D. Guillon, G. Rogez and B. Donnio, *Angew. Chem., Int. Ed.*, 2008, **47**, 490; I. M. Saez and J. W. Goodby, *Struct. Bonding*, 2008, **128**, 1.
36 M. J. Suh, V. Vien, S. Huh, Y. Kim and S. J. Kim, *Eur. J. Inorg. Chem.*, 2008, 686.
37 T. V. Larina, V. N. Ikorskii, N. T. Vasenin, V. F. Anufrienko, N. G. Naumov, E. V. Ostanina and V. E. Fedorov, *Russ. J. Coord. Chem.*, 2002, **28**, 554; C. Guilbaud, A. Deluzet, B. Domercq, P. Molinie, C. Coulon, K. Boubekeur and P. Batail, *Chem. Commun.*, 1999, 1867.
38 S. Suarez, O. Mamula, D. Imbert, C. Piguet and J. C. G. Bunzli, *Chem. Commun.*, 2003, 1226.

